Chapter 10 – Discharge Scenarios

Our objective in developing the discharge scenarios is to judge whether there are plausible and reasonable paths from vacuum fields to the desired NCSX target equilibrium. Our primary focus is the configuration li383_328. Much of the physics addressed here in pursuit of this goal is the evolution of the plasma poloidal flux. In addition to the vacuum transform, NCSX plasmas have significant toroidal current which is largely bootstrap driven. The plasma is heated by neutral beams and there is the associated neutral beam current drive. Finally, there is the directly controllable component, Ohmic current driven via a central solenoid. All contribute to the iota profile, some in competing ways. There is not a developed simulation tool for following flux evolution in 3-D; however, as the device is quasi-axisymmetric we expect the usual tokamak tools to provide an accurate guide. The discharge evolution will be followed using TRANSP, a 1 /2-D transport code with a high level of sophistication and maturity. The other major code used here is VMEC. For the most part VMEC will be used in its free-boundary mode with internal current and pressure profiles generated via TRANSP simulations, and searches for coil currents that retain attractive physics properties with these profiles.

There are four components to this task. First mapping the reference stellarator configuration into an 2-D "equivalent tokamak", called <NCSX>. Simulations are then developed to evolve the current profile from discharge initiation to the desired high beta state. Third, the profiles are mapped back into the 3-D configuration while solving the free-boundary equilibria to obtain the coil currents. Finally evaluating the physics predictions, notably kink stability, for these equilibria. Additionally, we present an alternative evolution of the plasma current buildup that avoids having the plasma edge pass through iota of 1/2.

10.1 Creating <NCSX>

As stated above the li383s configuration is the starting point for the analysis. The reference equilibrium is specified by its 3-D shape and its internal profiles (pressure and current). The first step is to remove the plasma pressure and internal current to obtain the vacuum iota. This iota is to be preserved as a current in <NCSX>. This seems the most straightforward approach, and implies the control is for essentially constant plasma shape. It is not a true requirement and an alternative is discussed in Section 10.4. It is the simplest choice. The next step is to make an axisymmetric equilibrium, retaining only the n=0 components of the reference. Here (and only here) VMEC is run in the mode where iota is preserved, rather than a current profile. As we have only axisymmetric terms this VMEC run then calculates the current profile needed to obtain this iota. This current profile is all that is needed from this calculation. This current, designated I_{EXT} is 321 kA for the R·B value of 2.05 T-m of the reference case. This transformation does not preserve aspect ratio nor plasma volume. We repeat, with a second axisymmetric calculation, keeping the n=0, m=0 term, but adjusting the n=0, m≠0 components by a single scale factor to restore the original aspect ratio, 4.37. In both cases we are keeping the value of toroidal flux at the boundary fixed at the reference equilibrium value. Since

we retain the vacuum iota, the major radius, the plasma volume and the edge toroidal flux, the new <NCSX> equilibrium has a new R·B, or B since R of <NCSX> = <R> of the stellarator equilibrium. With this prescription <NCSX> has R·B=1.84 T-m and R=1.42 m. This will produce profiles with I_P, and $\Phi(\rho=1)$ values which correctly map back into the stellarator with R·B =2.05. Since we are not able to retain the wobble of the magnetic axis, there is not a unique mapping to two dimensions. If we think of iota in terms of poloidal and toroidal currents, $\iota \propto R^2 I_{TOR} / (a^2 I_{POL}) = R I_{TOR} / (a^2 B) = R I_{TOR} / \Phi_{edge}$. Matching ι at a specified Φ_{edge} with I_{TOR} constrained, uniquely, allows for only B_ϕ as the freedom to preserve the boundary iota value. The <NCSX> equilibrium flux surfaces and current profile are shown in Figure 10-1.

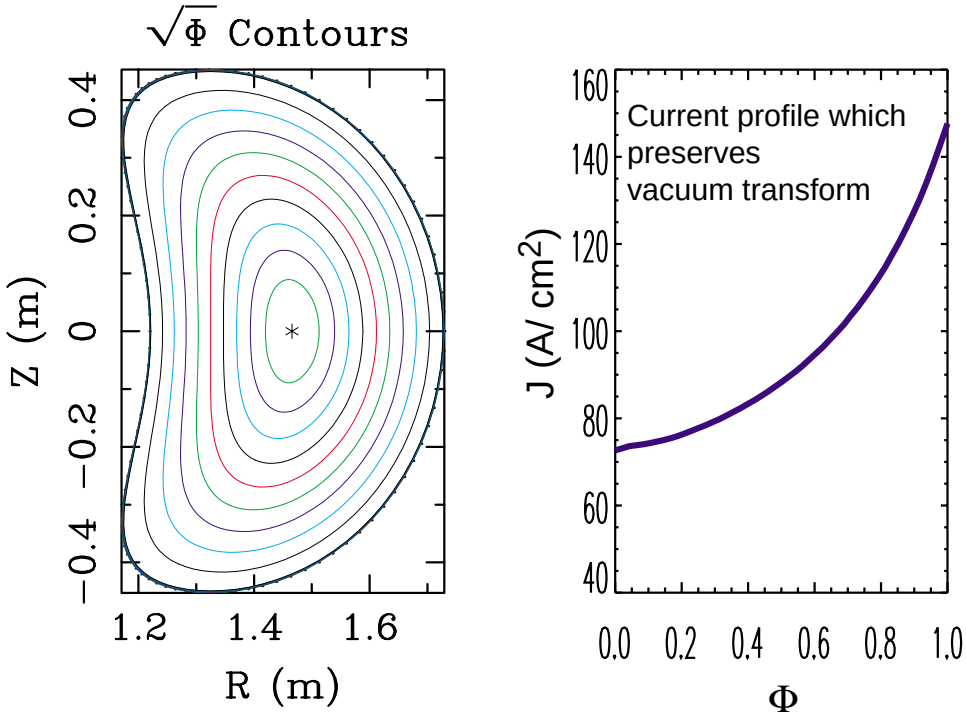

Figure 10-1 (a). Flux surfaces for the axisymmetric components of the shape of the target equilibrium, li383_328, at β=0, I_p=0 and (b). the toroidal current density required to produce the vacuum transform in the absence of 3D shaping

10.2 Discharge Evolution Modeling

The modeling of the current profile is done using TRANSP. The evolution of the plasma pressure components (T_i, T_e, n_e, and Z_{eff}) are specified in a way consistent with the predictions of Chapter 8. The plasma current has two distinct components: The 321 kA equivalent of the vacuum iota is specified to be lower hybrid driven current (LHCD). The unique aspect of LHCD is that TRANSP assumes a power source maintains this current and it does not diffuse. Other physics assumptions of importance are using the NCLASS [1] models for bootstrap current and neoclassical resistivity. The NCLASS calculations, which do more accurate (numerical) integrals of the distribution function

result in about a 13 % decrease in bootstrap current, when compared to the usual analytic approximations. While neoclassical resistivity is similar outside the half-radius, near the axis the NCLASS calculation results in a 40% increase. Before proceeding we need to describe this use of TRANSP; TRANSP is an analysis code, not really a simulator. The simulations are done iteratively: do a run, look at results, change something and do it again -- very much like running a tokamak. This will be obvious in the plasma current. In order to maintain a current profile that is approximately constant in time, it is quite important to minimize the Ohmic current during startup. When the plasma is cold, the current diffuses rapidly to the core. Once the plasma heats it will take a very long time to dissipate the Ohmic flux. The plasma current waveform, $I_P(t)$, represents a number of iterations where the old waveform is replaced with a new one which is the integral of the non-Ohmic current. Of course, this changes the β_P, leading to a different bootstrap current. The change in I_P will also change the neutral beam current drive (NBCD). Additionally, the balance of the neutral beams is adjusted so that the counter losses are compensated by a lower coinjected power. This is done so the effect of NBCD on central iota is not too severe, while overall the NBCD is not too negative. While the NCSX program will include an upgrade of the neutral beams to long pulse, initially they will be limited to a pulse length of 0.3 s. It is desirable to develop a scenario consistent with initial operation - despite the long skin time of the plasma. This is not the only simulation we have done, it is the one at highest electron temperature, and thus the most difficult. The T_e profile is chosen to be roughly consistent with the confinement predictions of Chapter 8. The electron density profile is like that used in Chapter 8, but the overall magnitude is adjusted to produce the desired β_T. This differs from Chapter 8 in that the fast ion beta is about 25% of the total. The profiles are rather broad and this expectation is discussed below. Also, β_T is the convention tokamak definition, whereas in the stellarator β is <p> divided by the $\langle B \rangle^2$, the volume-averaged total field A typically 0.92 typical difference in NCSX is $B_{0,0}/\langle B \rangle = 1.05$.

As the design goal is a quasi-axisymmetric device, it is very useful to examine <NCSX> in some detail. Usually, one would begin with the I_P waveform. However, our waveform is the resultant of the specified pressure profile, a discussed above, so we shall begin with Figure 10-2, the assumed profiles. (In the case of T_i the assumed multiplier on neoclassical transport.) The electron temperature is about 2.2 keV on axis in the high beta phase, starting from 50 eV at t=0. (Because of the care needed in initializing TRANSP at near-vacuum conditions, the plasma start is at 20 ms when the current ramp begins. The ion temperature, calculated from neo-classical conductivity with a multiplier (3) that results in the expected central value.

The density profile is consistent with observations in tokamaks and stellarators operating at this field value. As a guess, Z_{eff} is fixed at 2 in the center and the profile is set to rise modestly with time.

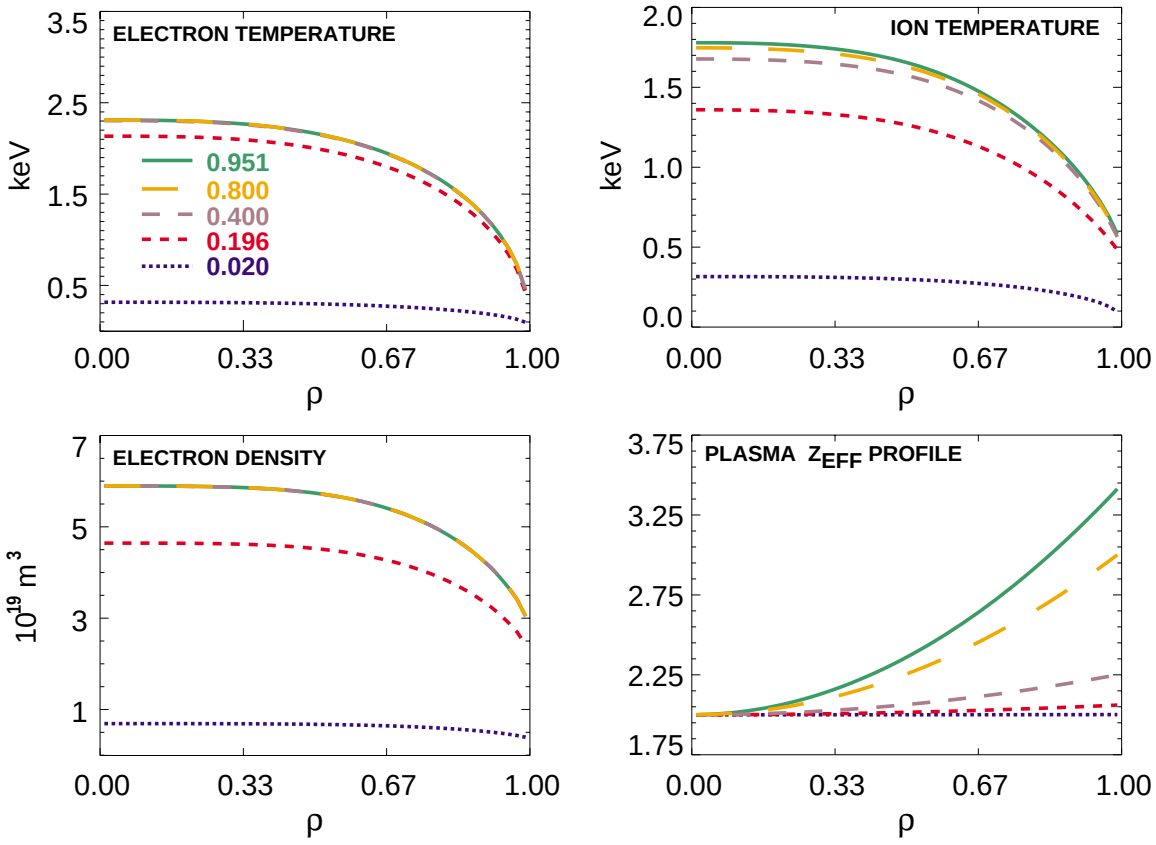

Figure 10-2. Thermal plasma components; T_e, T_i, n_e, and Z_{eff}. at selected times

The profiles along with electron collisionality determine the bootstrap current profiles. The resulting collisionalities, ν_{*i}, and ν_{*e} are shown in Figure 10-3 for the high β phase.

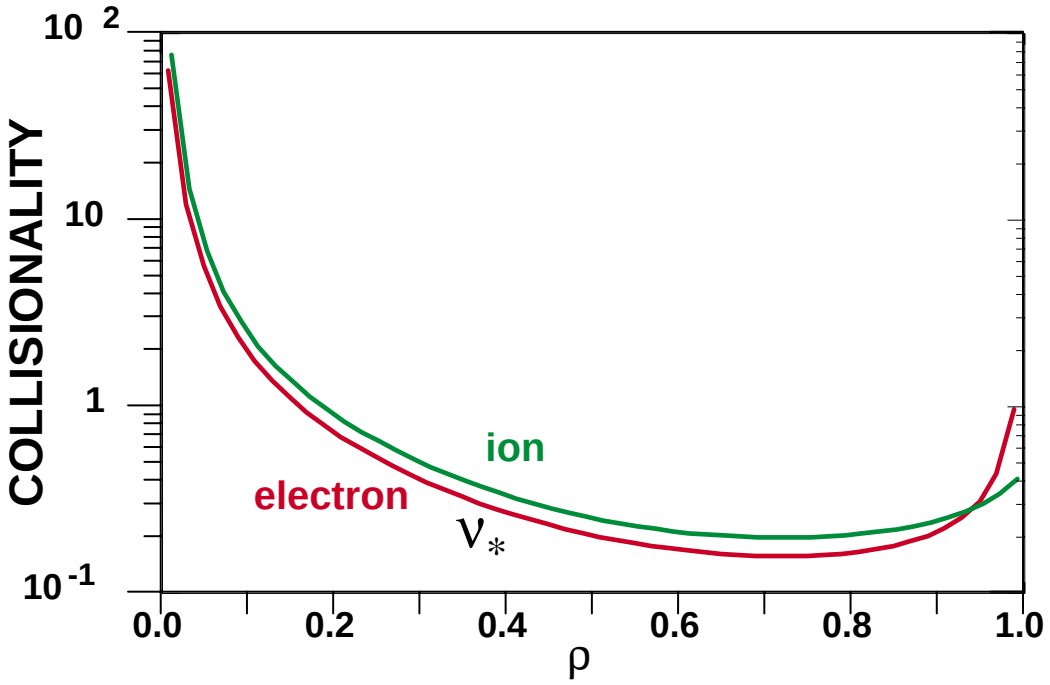

Figure 10-3. Electron and ion collisionalities at 0.4 s

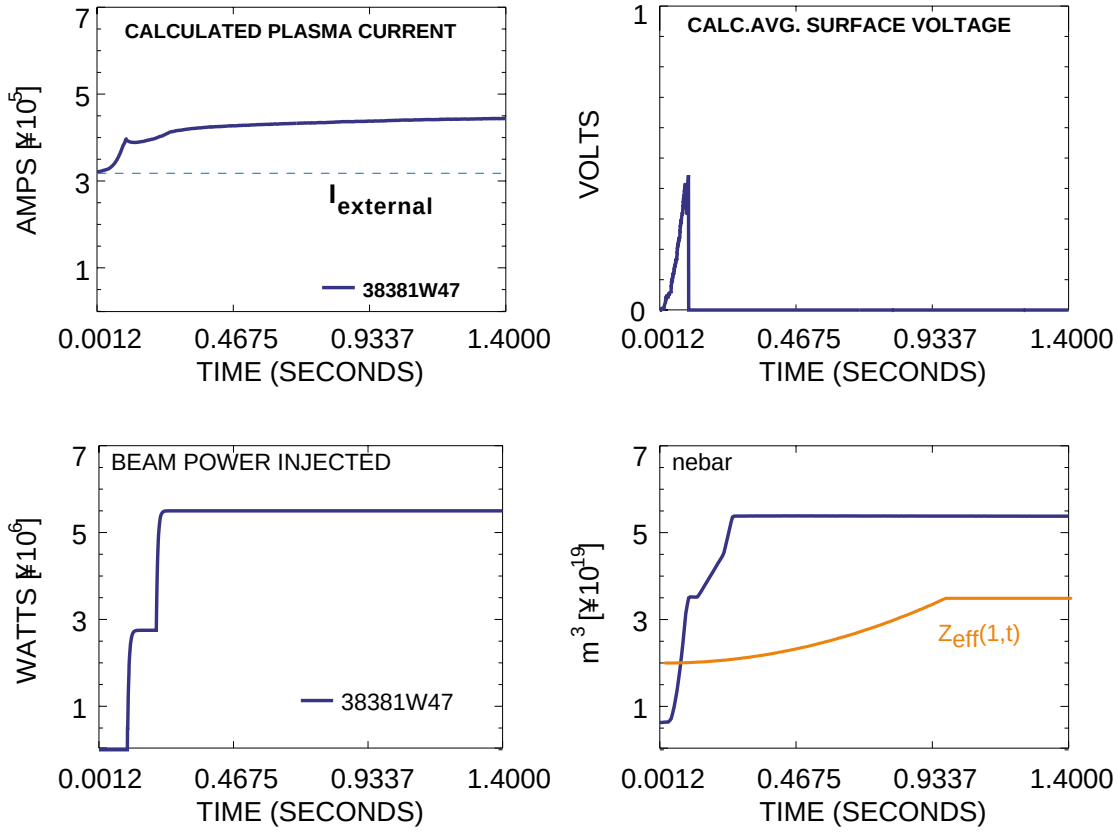

Figure 10-4. Evolution of plasma current, surface voltage, P_{inj}, density and Z_{eff}

Figure 10-4 shows the evolution of primary quantities. As already stated, the current rise is set to match the rise of driven current as closely as possible. The starting value of 321 kA is the I_{EXT} that gives the correct vacuum transform. The OH circuit is switched from current to voltage control as early as possible, near the time when NBI begins. Unlike a tokamak where there is a need to breakdown without pre-existing surfaces, this device has closed surfaces at t=0. Thus we would expect the voltage requirement to be accurately predicted here. The surface voltage only reaches a peak value of less than 1 volt, which should not present any difficulty The injected power is begun as soon as the plasma current reaches its approximate flat top in steps of 2.75 MW. The beams are paired, co & counter – unbalanced injection is not possible without severe effects on iota. The power balance is a compromise between reversing iota in the center of the plasma and minimizing the overall negative contribution of NBCD to the plasma current. Line-averaged density is programmed for the desired β.

Parenthetically, in earlier work, assuming a colder plasma (Te(0) ~ 1 keV) it was sufficient to raise the plasma current at 2 MA/s to achieve an equilibrated, bootstrap-driven plasma at similar beta in 0.4 s. This ramp rate produced an Ohmic current profile sufficiently similar to the final bootstrap current to make this possible. At the higher temperatures current equilibration is, of course much slower. Those plasmas require about twice the voltage in the current ramp as this case.

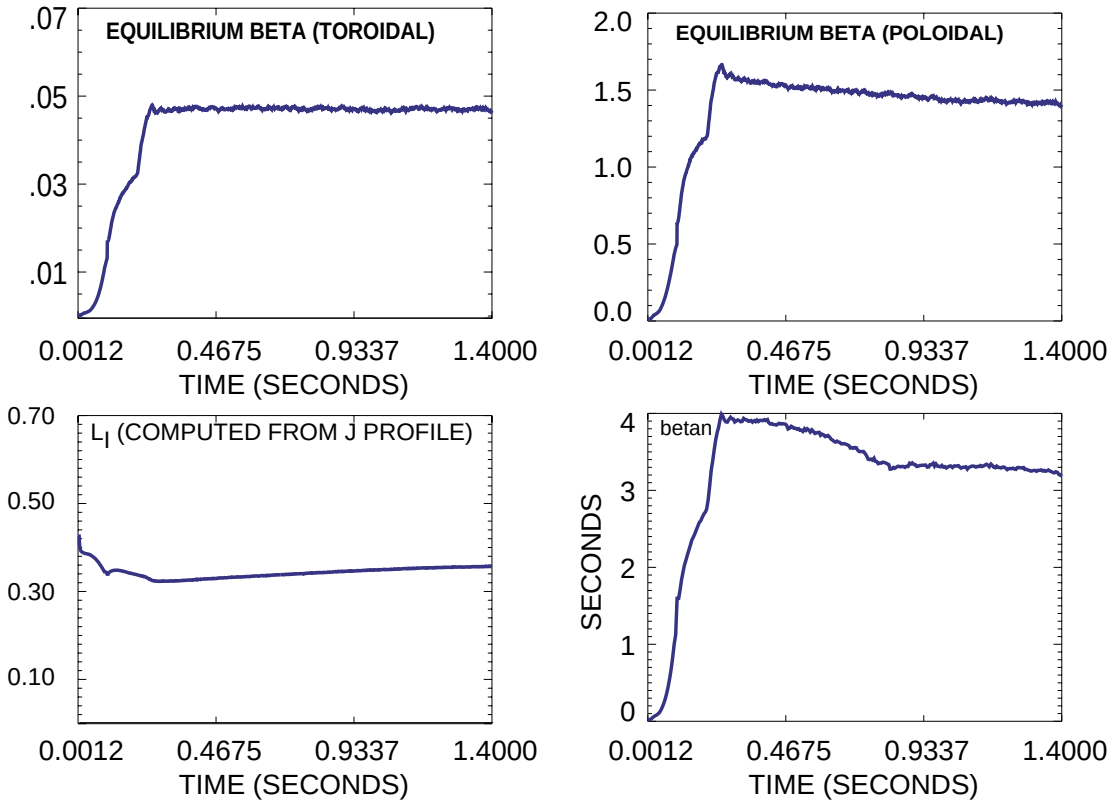

Figure 10-5. Discharge evolution; betas and plasma inductivity

β_T is chosen by control of the density to be that (4.8%) which corresponds to β=4.25 % in the stellarator. This corresponds to $\beta_P \approx 1.5$, as shown in Figure 10-5. For comparison to the tokamak, we show β_N and ℓ_i. In a tokamak, the kink stability limit (no wall) is approximately given by $\beta_N = 4 \cdot \ell_i$ Here we will obtain kink stability at $\approx 10 \cdot \ell_i$.

The calculation of the evolution of the current profile is the primary purpose of modeling the discharge evolution with TRANSP. The current profile comes quite close to being stationary in a 0.4 s pulse, consistent with the initial NB pulse length of 0.3 s, meeting the goal mentioned above. A true equilibration (flat voltage profile) would take quite a long time and require the planned beam upgrade. It is plausible, but not entirely clear, that the evolution shown hear could be achieved in practice. (We will touch on plasma control in Section 10.5.) The current densities are shown in Figure 10-6. Clearly the LHCD (external transform) is the dominant term. The bootstrap current is somewhat less than that shown in other chapters because the thermal pressure is 75% of the total (Figure 10-7) and the fast ions do not contribute significantly to the bootstrap current. While the NBCD from the "balanced" beams is small overall, it has a pronounced effect in the core, tending to increase iota because the co-injected ions are better confined. The dependence of the screening factor on Z_{eff} and aspect ratio is shown in Figure 10-8. For Z_{eff} in the expected range of 1 to 2.5 control of central iota will be an exacting task. The central value is quite important; for values less than 1.4 the effects of NBCD on central

iota are negligible, whereas at central values of 2 the effects are marked and this has been the principal determinant how the NBCD and OHCD are competed, as discussed in more detail below. Co-injection orbit losses are about 18% and counter-injection losses are about 30% (Chapter 7).

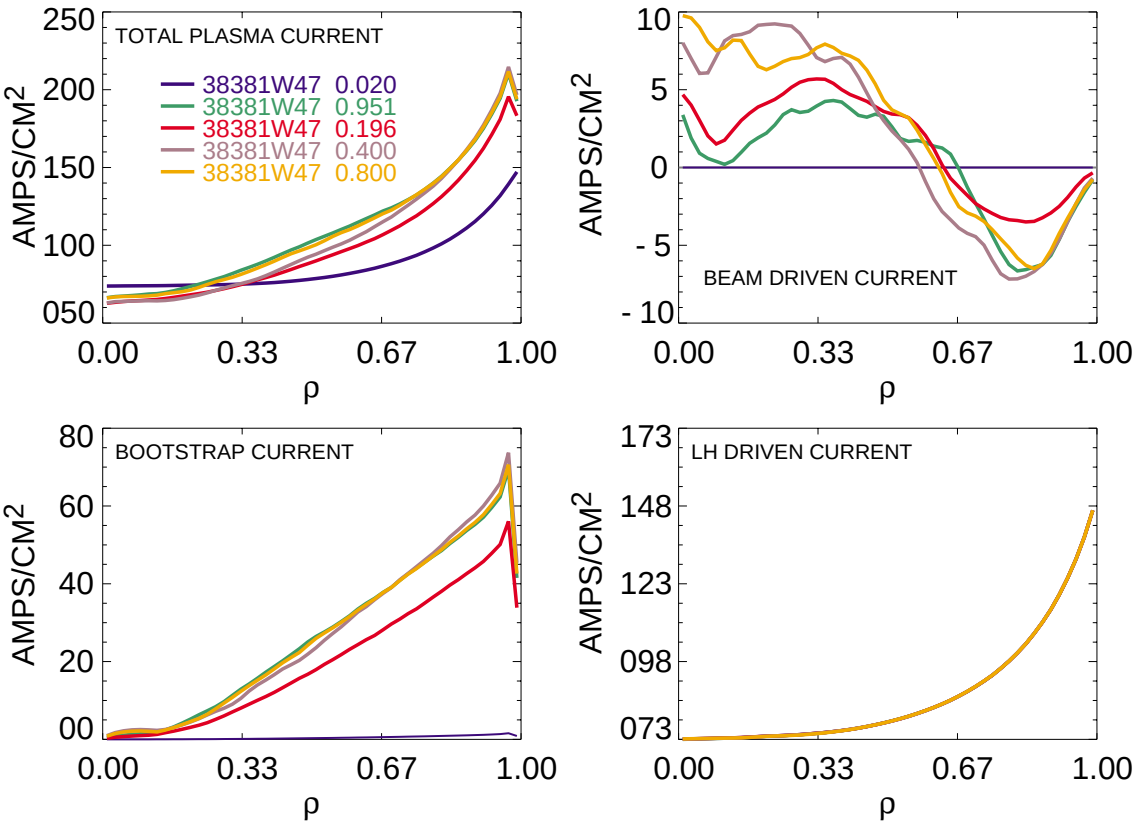

Figure 10-6. Components of the current profile at selected times

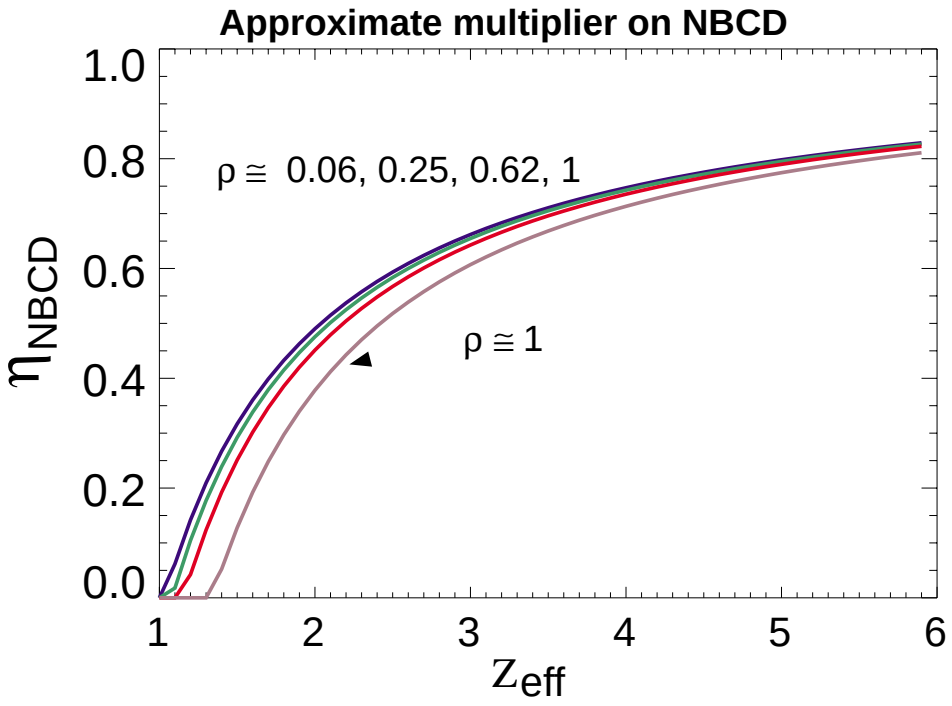

Figure 10-7. NBCD screening; $J_{NBCD} \approx n_f \; v_b \; \lambda\eta$

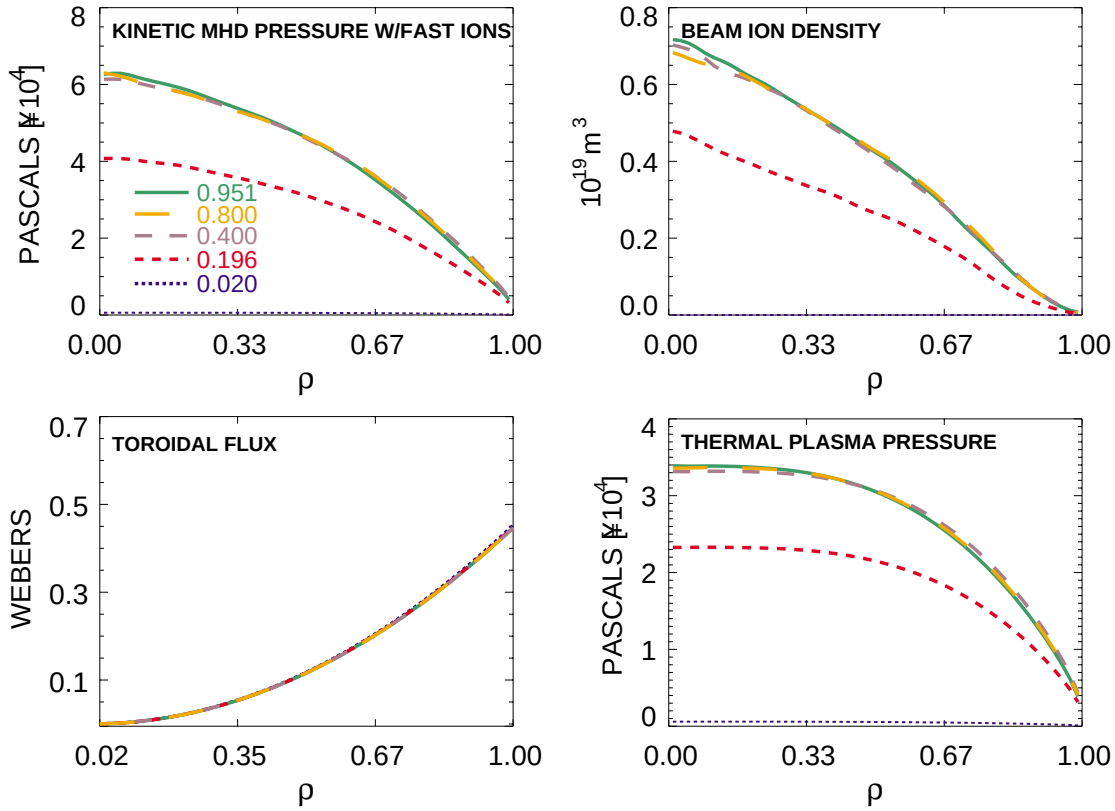

Figure 10-8. Components of the pressure profile at selected times

Our objective is to assess whether we can reasonably expect to obtain an iota profile which is reasonably consistent with the target equilibrium and to judge how much time is required to do so. The answer, in the affirmative, is shown in Figure 10-9 below. The loop voltage shows little sign of decay. Suitable averaging over the plasma cross section does show that after about 0.3 sec there is a decrease. However, the source of the voltage is the inductive reaction to internal driven currents and control of surface voltage is only a weak control on the loop voltage. The Z_{eff} profile is still changing gradually until t=1.0 s (Figure 10-5). At 1.4 s, the end of the simulation, there is still voltage churning with continuing change in iota. Recall that the plasma profiles are fixed. If the confinement depends on the plasma current, as expected, the time will be lengthened. Nevertheless, with adequate knowledge of the plasma currents and robust plasma control, maintaining a qualitatively similar iota over the beam-heating phase of a 0.4 s pulse is possible.

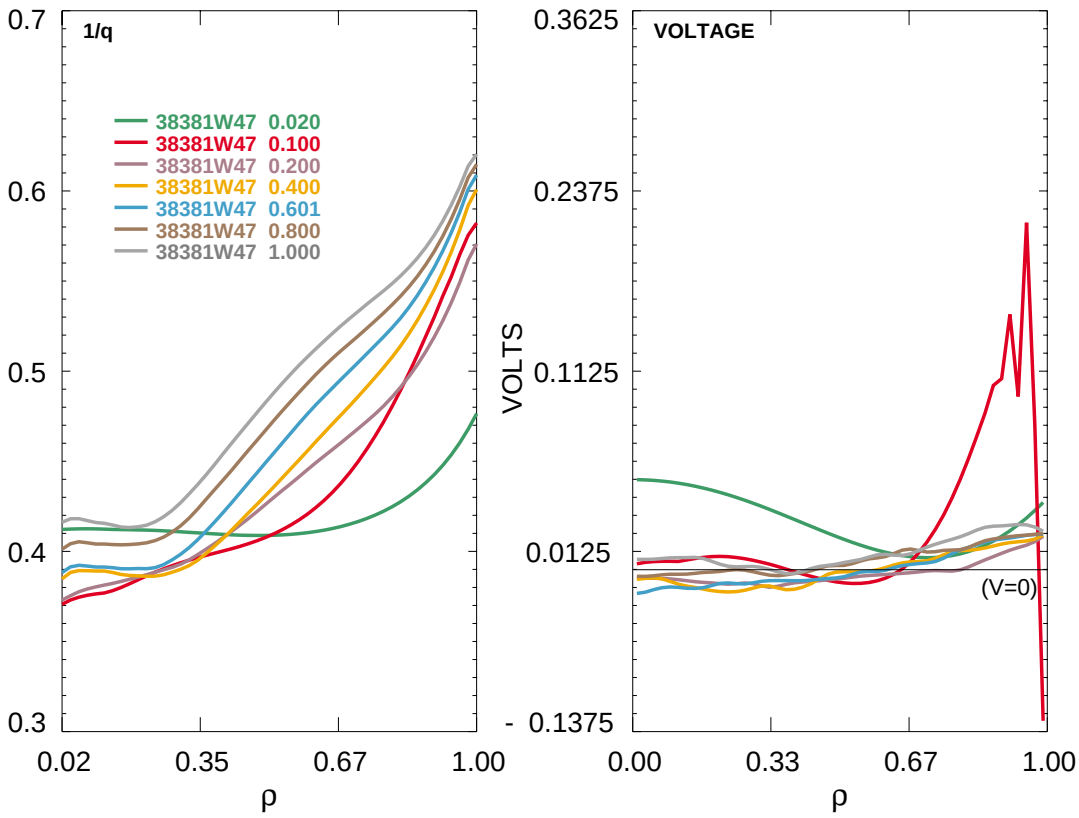

Figure 10-9. Iota and voltage profiles at selected times

While the loop voltage settles to quite a small value, there is an issue of how to define "small" when a goal is to preserve iota. To examine this we form the components of the internal voltage, $\eta \cdot J \cdot 2\pi R$ for the current components as a local (surface-averaged) quantity. Additionally we have run this simulation longer to see the decay time. These results are shown in Figure 10-10 below along with the components of total current. By 3 sec the Ohmic current has decayed virtually to zero. The integral neutral beam current is quite near zero throughout the discharge. The voltages are plotted at ρ=0.33. To allow clarity in the figure we plot the negative of the Ohmic voltage. These voltage signals are quite noisy as a result of Monte Carlo beam deposition and are heavily smoothed. The Ohmic voltage provides reasonably good cancellation of the neutral beam voltage until about 1 s. At that time, to preserve the shape of iota the co-injected beams should be reduced further eliminating the positive central current shown in Figure 10-6. This will result in a decrease of the total current by several kA.

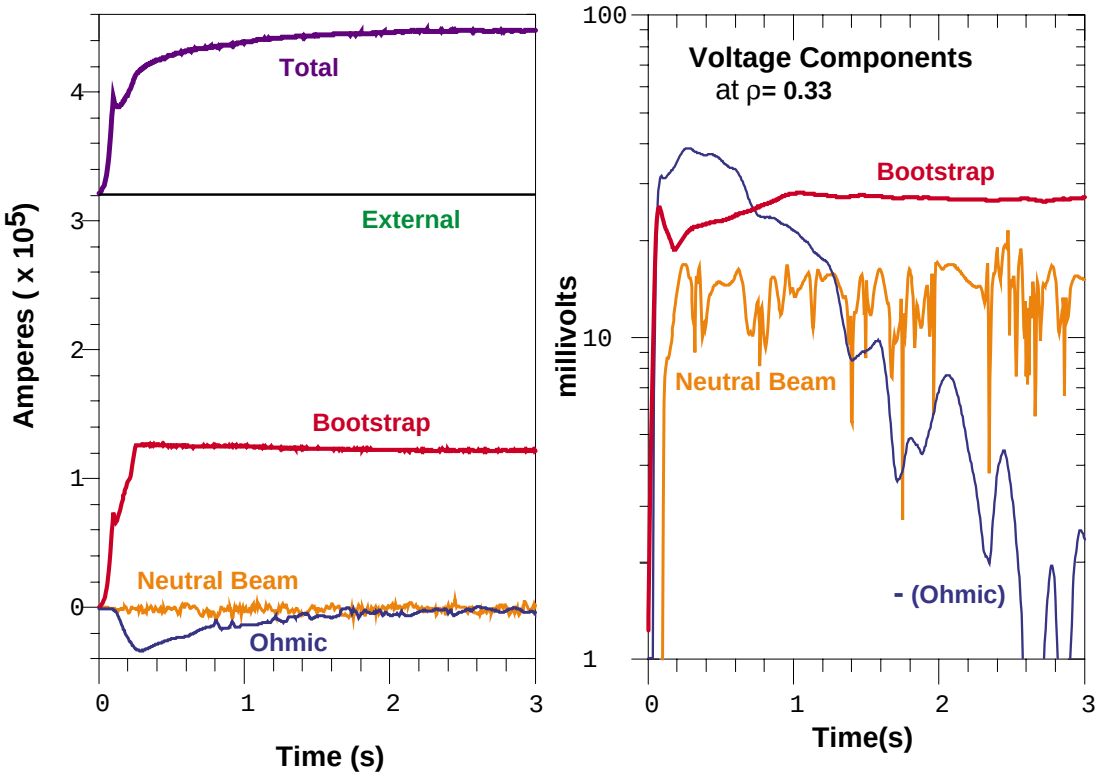

Figure 10-10. Components of toroidal l current and local toroidal voltage vs. time

Whether the confinement will be good enough to make this plasma is, of course, unknown. Beta studies may require that we operate at lower field. This would ease the problem of current control by reducing the resistive diffusion time. Estimates of confinement based on popular scaling are presented in Figure 10-11 below. τ_E^* is (W/(P_{in}-dW/dt); τ_E^{D3J} is D3D-JET scaling [2]. The enhancement factors are somewhat higher than that shown in Chapter 8 as required to achieve this beta. The biggest factor is a larger B_T = 1.4 T (instead of 1.2 T in Chapter 8). Other factors are lower bootstrap current, resulting from the non-thermal component of beta, the difference between B_{T0} and <B> in normalization of tokamak and stellarator betas and other similar small factors. We would judge the discharge presented here as energetically plausible.

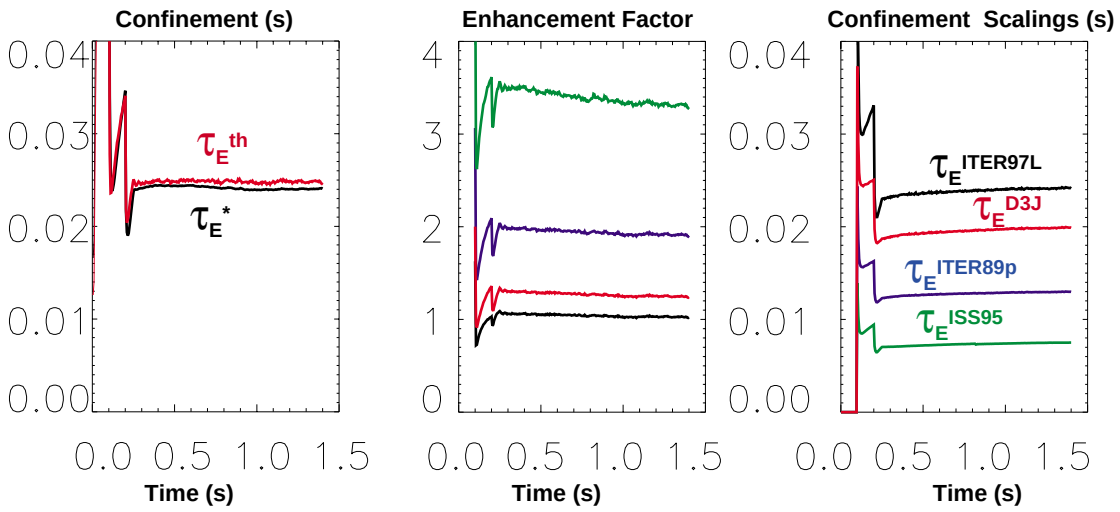

Figure 10-11. Confinement Times

10.3 Repatriation of 2-D results to the stellarator

Having obtained a self-consistent evolution of pressure and current density, we need to follow this path in a sequence of 3D free-boundary equilibria. The input profile functions for VMEC are the pressure, p(s) and flux-surface averaged current profile, I'(s), where $s=\rho^2$. $P(\rho)$, and $[\langle J\rangle(\rho) - \langle J_{LH}\rangle(\rho)]$ are extracted from the TRANSP for multiple time slices and fit to obtain the desired input functions using SVD techniques. The 3-D free-boundary equilibria are generated by an optimization process discussed in Chapter 2. We will first address the 0907a2 coil set (a2 => set of 7 PF coils). Later we will discuss progress with other coil sets that have presented difficulties.

Our first task is to obtain a converged equilibrium at any time in the discharge. The coil currents need to be reasonably consistent with the plasma. Changing beta or plasma current without changing coil currents leads to poorly converged results. This is most easily done at a time corresponding to conditions near the reference equilibrium. For each time slice we optimize as described below and then use the resulting coil currents (and magnetic axis) in the next time slice. This is repeated until all slices are done. We need a first slice with a well-converged equilibrium. After that calculation is largely an automated process of optimization with an initial guess form the previous case. A failure simply means a higher density of time slices is required.

Using the 0907a2 set also created some problem in that we could not obtain kink stability at the aspect ratio of 4.37. We did obtain good results at a lower aspect ratio, 4.12. This type of behavior is discussed in Chapter 2. This means our simulation results will be in error by about 6%, the change in the gradient scale length. In particular the bootstrap current density will be overestimated by about 6% and the integral, I_{BS} is underestimated by the same 6%. Also, the plasmas do not quite fit in the nominal plasma facing component boundary. The plasma volume was increased by about 12% by the aspect ratio change.) These details are not of concern until a coil set is finalized.

For the "W47" cases we did a full optimization over aspect ratio, R·B, quasi-symmetry, and the N=0 & N=1 families of ideal (no wall) kink instabilities. No attempt is made to regularize the coil currents or force the plasma to fit within the vessel. Results from 40 to 840 ms are presented in Table 10-1. A growth rate for the kink of $< 1 \cdot 10^{-4}$ is considered negligible, that is, with minor changes in discharge programming it can be avoided. This is satisfied for all except the 420 ms case, which comes quite close. χ^2_{Bmn} of the reference plasma is 0.015 and values less than .04 are not expected to be deleterious to confinement. The last column displays radial zones that are ballooning unstable. (1 the axis and 49 the boundary are not evaluated. Instability is restricted to a few zones near the axis and the boundary). Ballooning is evaluated on field lines beginning both at $N_{fp}\phi = 0°$ and 60°.

Time (ms)	VV distance (m)	A	<β>	I_P	N=1 & N=0 Max $\gamma\tau_A$ x10^{-5}	χ^2_{Bmn}	Ballooning unstable zones
0041	-0.2437	4.118	0.001	6590	3.00	0.0291	0
0061	-0.0507	4.123	0.002	18580	0	0.0303	0
0081	-0.0048	4.123	0.006	42860	0	0.0337	0
0106	-0.0109	4.123	0.016	71860	1.38	0.0327	0
0131	-0.0129	4.123	0.022	68340	8.40	0.0324	2
0151	-0.0124	4.123	0.025	69980	9.11	0.0334	2
0211	-0.0142	4.122	0.032	80700	7.52	0.0356	2,3
0315	-0.0138	4.123	0.042	100200	6.10	0.0407	2,3
0420	-0.0140	4.122	0.042	105500	10.7	0.0515	2,3
0524	-0.0160	4.122	0.042	109000	8.31	0.0378	2,3,48
0525	-0.0153	4.122	0.042	109000	7.45	0.0353	2,3
0630	-0.0131	4.123	0.042	111800	5.70	0.0300	2.3.48
0735	0.0007	4.132	0.043	114000	3.18	0.0298	2,3,48
0842	-0.0353	4.122	0.043	116900	5.74	0.0330	2,3,48

Table 10-1. Optimization Results; Case bB3.0907a2_38381W47

It is of interest to examine the plasma shapes resulting from this process. These are shown in Figure 10-12. The important point is that 12 optimizations return virtually identical shapes. The optimization at 40 ms (20 ms after the beginning of the I_P ramp) is unlikely to be of importance. The optimization at 524 ms, continued further as 525 ms is driven by ballooning stability, which is always a few zones near the axis and boundary. Again, unlikely to be of importance. The conclusion is that control of the plasma boundary will maintain the transport and stability properties. For the actual operation of the device, this is a quite favorable result.

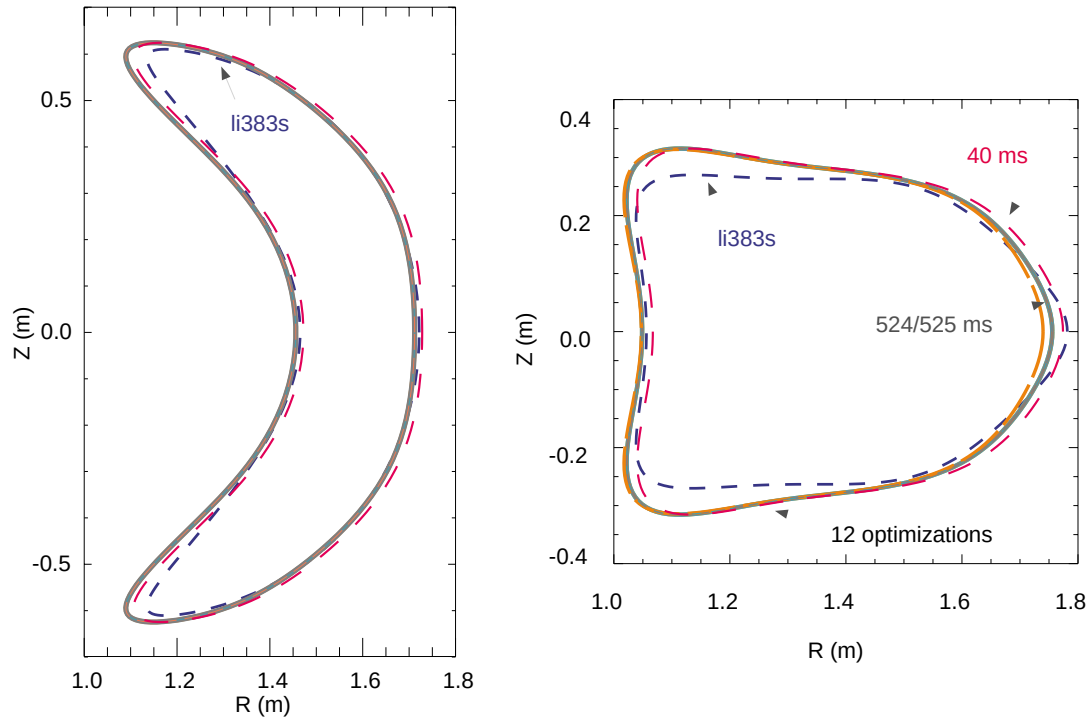

Figure 10-12. Optimized Shapes, $N_{fp}\phi = 0°$ and 180°

There has been no effort to regularize coil currents. Nevertheless, the modular coils do not make any severe excursions during 840 ms (Figure 10-13). The toroidal field does so at the first time slice, where the shape departs from the norm. This could likely be avoided, as could the large interference with the nominal PFC boundary. Beginning at 840 ms the toroidal field again departs the norm. After that we did not obtain attractive solutions. While we have not attempted to correct the situation, we think it likely that the change in central iota is the root cause of the changes in optimization results. As mentioned above, correction requires a further adjustment of the co/ctr beam balance .We should consider adding other heating such as RF after initial operation with 2 beams, to avoid additional beam-driven currents.

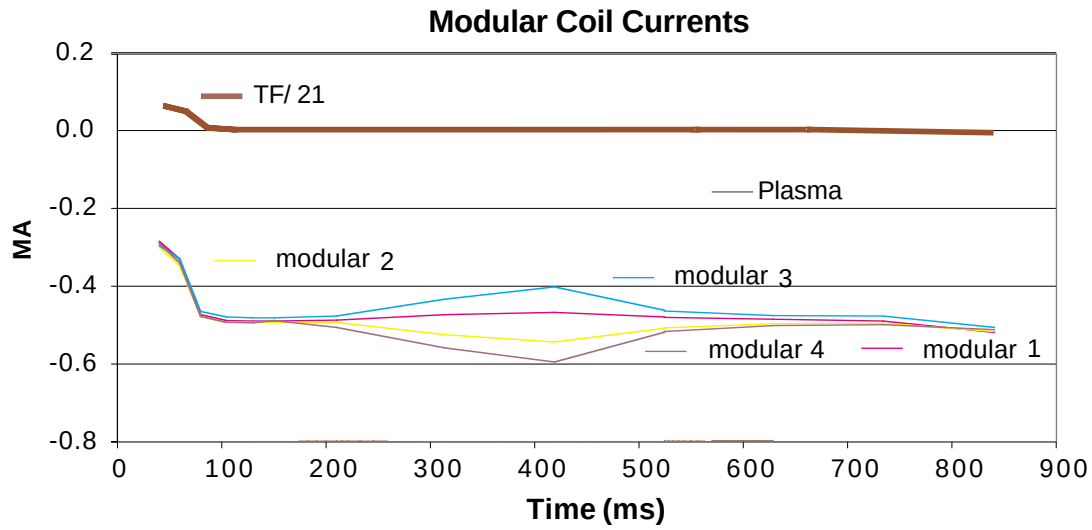

Figure 10-13. Modular Coil Currents for Optimized Shapes (0907a2)

The situation for the poloidal coils (Figure 10-14) is still less likely to be an accurate portrayal of an optimized system. This set of 7 poloidal coil pairs is simply putting them everywhere there is space, allowing them to conflict with each other, but yield favorable solutions. This is a proper starting point, but reducing the PF set and finding optimal coils requires finalizing the modular coil set, a task that is still in progress. The figure represents a part of this data set, and for this reason we include it. We do not expect it to be representative of the final design.

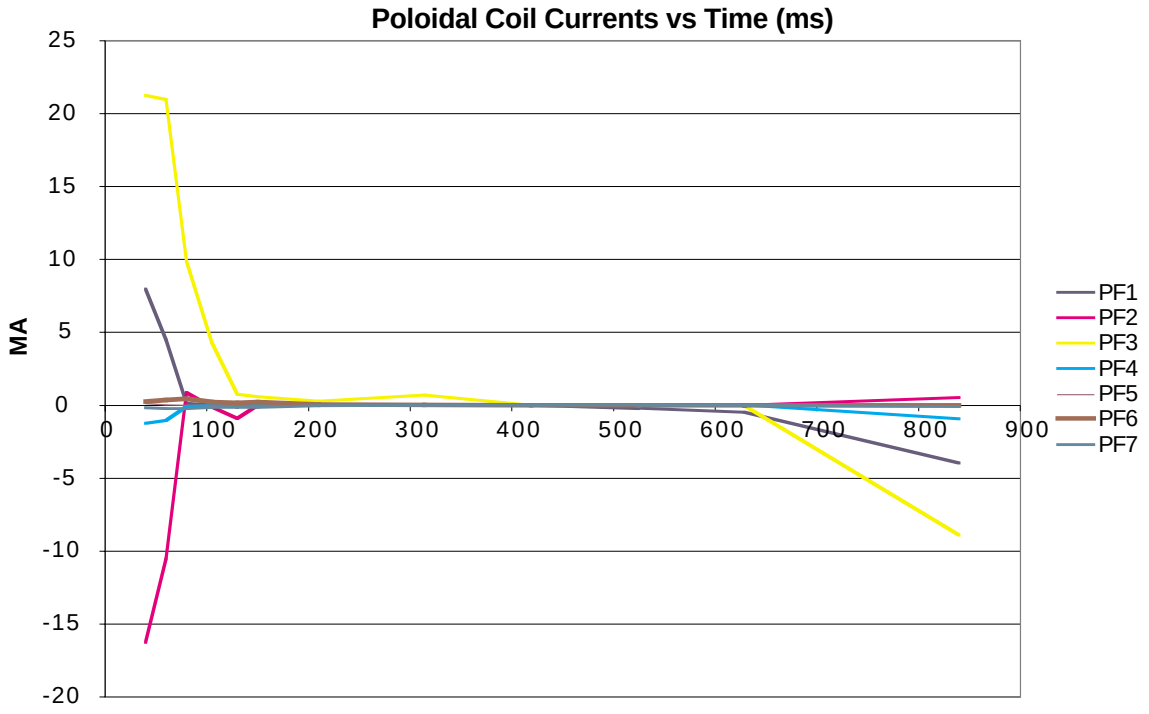

Figure 10-14. Poloidal Coil Currents for Optimized Shapes (0907a2)

The distinction between 0907a2 and other coil sets we have tried to work with is that 0907a2 does not have the outer legs of certain coils moved radially to provide neutral beam access. Our most diligent attempt was the 1017 modular coils with the a2 poloidal coil set – 1017a2. We were unsuccessful at obtaining a good solution. In particular, the stabilization of the kink family was not possible and attempting to do so drove the shape to have unattractive features. Additionally, when we tried to lower beta the coil set also produced unattractive shapes. Simply to obtain convergent VMEC solutions constraining only the target shape required a higher density of time slices than was needed for the 0907a2 coil set. With the 0907a2 coil set the methodology of either optimizing on a shape or optimizing the physics directly seems to yield good and similar results. Obtaining one good result and using this to iteratively do all the time slices works well with either It is tempting to interpret these failures as physically meaningful but this is dubious. The optimization by gradient search is prone to encountering local minima and the sensitivity to various starting points we have observed in these attempts suggests this may well be the problem. It remains a strong possibility that the methodology is simply unsuitable to coil sets other than 0907a2 and we will need to find a better approach. We have not been entirely unsuccessful, in that some solutions with satisfactory physics have been obtained. However in these cases the optimizer had managed to elude our intent and raise R·B to 2.2, lowering beta to 3.6%.

At the time of writing this final version of chapter 10, we have had the first success with the 1017a2 coil set. The procedural changes have been slight, making it very likely the entire sequence will yield stable results. This slice corresponds is 525 ms in Table 10-1The results as an addendum to Table 10-1 is

0525	-0.0133	4.122	0.0411	109000	5.87	0.0503	2,3

The kink stability is now adequate, and the quasi-symmetry a bit less than desired. These are upper bounds as the calculation is still in progress. This result does increase our confidence that the issue is methodology rather than intrinsic properties of the coil set. Further work is required to achieve satisfactory resolution on the adequacy of these coils.

10.4 A High IOTA Startup

The evolution described in the previous section appears satisfactory. As discussed in Chapter 6, Δ' calculations (in the cylindrical limit) indicate the n/m=1/2 island width is always small, a few percent of the minor radius or less. Nevertheless there is some concern, based on W7AS results [3], that an evolution which has ι=1/2 passing through the plasma boundary may experience problems of resistive instability leading to disruption. An alternative is to start the plasma with a different shape. In Figure 10-15 the shapes and iota progression are shown. At 105 ms the plasma has returned to the conditions of the case discussed above. The profiles are as in the previous cases. ι remains always above 1/2 with a constraint that the transform not be shearless. For the

most part, they fit in the vessel's notional plasma facing components. All are at R·B = 2.05 T. The quasi-symmetry and stability are shown in Table 10-2.

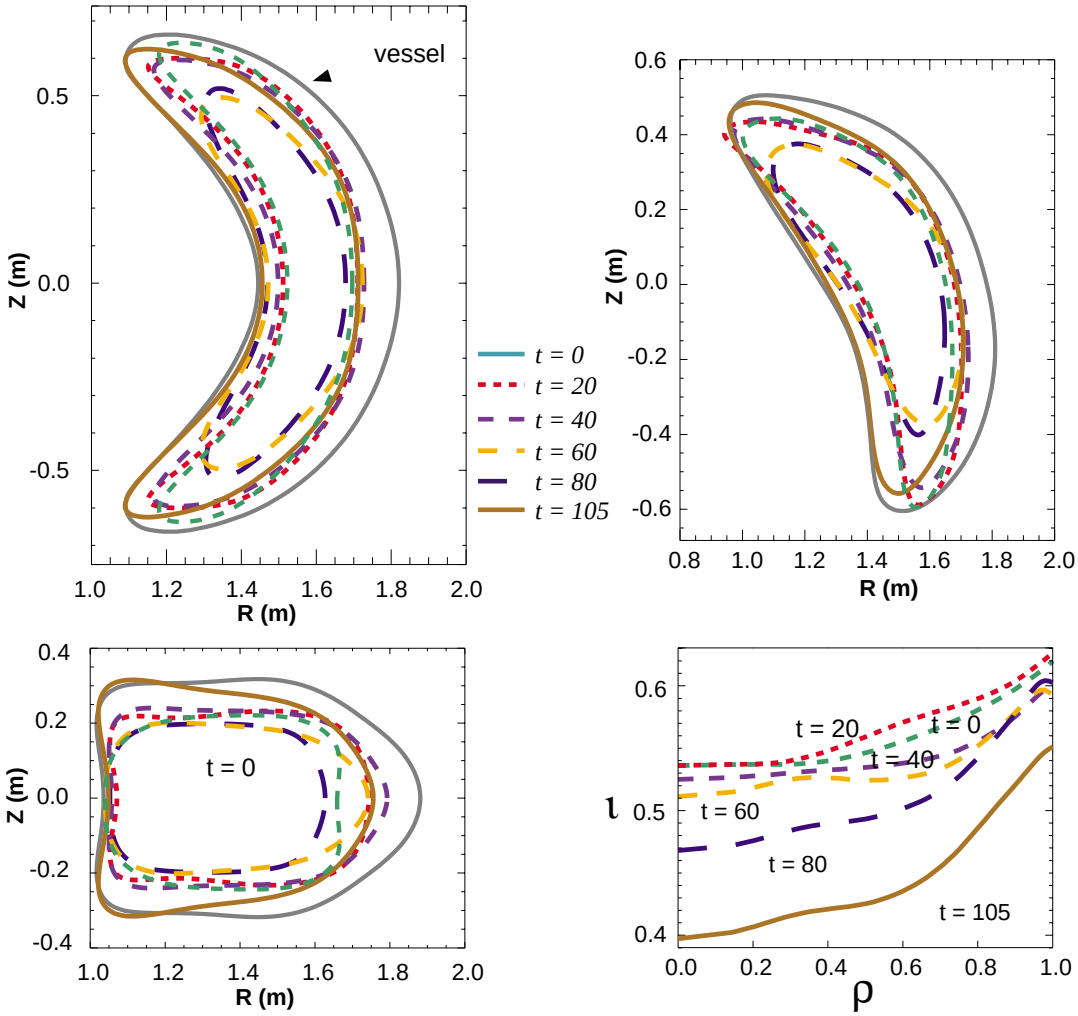

Figure 10-15. Plasma shapes at discharge initiation and during the current ramp which avoid ι=1/2 at the boundary. Shapes are shown at $N_{\phi\pi}$ ϕ= 0, π/4 and π/2

Time (ms)	Plasma Current (A)	χ^2_{Bmn}	λ_{KINK}	Balloon unstable zones
0	2280	0.053	vacuum	vacuum
20	6570	0.044	~ vacuum	0
40	18500	0.032	$4.1\ 10^{-7}$	0
60	42900	0.024	$2.7\ 10^{-5}$	13 , 14
80	71900	0.019	$5.2\ 10^{-5}$	0
105	109200	0.033	$1.4\ 10^{-5}$	0

Table 10-2

This series of optimizations has led to an odd sequence of shape, but makes the point that such a startup is within the capabilities of the coil set. Currents for the modular coils are shown in Figure10-16. In spite of the shape variations, there is little change in the modular coil currents.

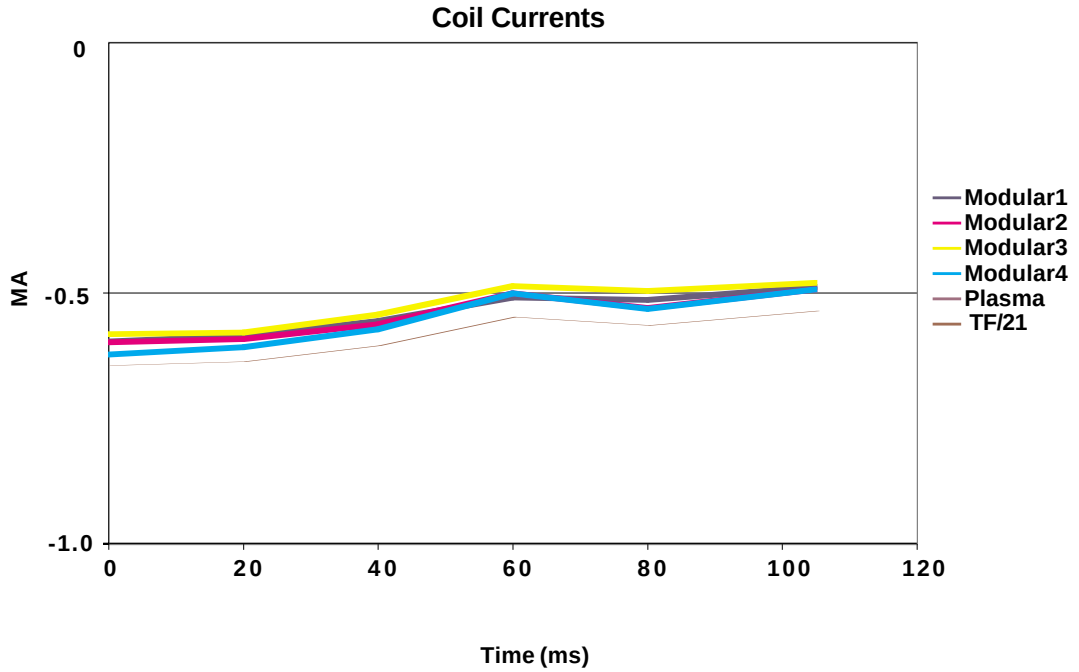

Figure 10-16. Modular Coil Currents for High iota startup

10.5 Discussion and Conclusions

Proceeding from the reference stellarator equilibrium we have constructed an "equivalent tokamak" with the vacuum transform represented as an LHCD current profile. Using this starting point in TRANSP we have evolved the plasma pressure and, along with the pressure, the self-consistent current profile to reach the target β. Such a plasma may require H-mode operation at B=1.4 T, but less confinement would be adequate at lower fields. The simulations include fast ion effects, and we find that care must be taken to account for NBCD, particularly its effect on central iota. Tailoring the $I_P(t)$ waveform and balancing the beams to account for increase losses in the counter direction achieves a nearly stationary iota profile from the start on NBI.

Analysis of the simulation profiles in 3-D yields a stable operating path to the target plasma while preserving good quasi-symmetry. These results are summarized in Table 10-2. Adequate stability to both kink and ballooning modes was found. This was done with the 0907a2 coil set. Even then, the initial aspect ratio did not yield good results and a further change from A=4.37 to A=4.12 was required. In earlier work which ranged

to $\beta\sim$ 3% this was not necessary. This change was driven by the requirement for stability to low n modes. Optimizations such as done here don't really exclude the 1017 coil set or the higher aspect ratio of 4.37. These optimizations can be sensitive to the exact process used, initial conditions, the order in which optimizations are done, etc. We have not find these solutions, but cannot say that they do not exist. As discussed in Section 10.3, the most recent results make us optimistic that better solutions will be found.

An alternative startup scenario, avoiding the ι=1/2 surface passing through the edge of the plasma. Cylindrical Δ' calculations indicate that the width for the m=3, n=6 island will be small, suggesting this may not be necessary (Chapter 6).

The scenario developed here assumes the existence of a rather sophisticated plasma control system and Ohmic circuit. Such a system would be a 3-D version of something like the D3D PCS. Thus it should not be viewed a radical advance, rather an extension of previous work in tokamaks. As a precursor to the control system it is necessary to undertake a study of 3-D equilibrium reconstruction. The question to be answered is how much profile information can be extracted from magnetic diagnostics and which diagnostics, and how many radial layers, are required to allow optimal control. For example, it is known that in 2-D ℓ_i cannot be determined from magnetics in a circular plasma, but configurations with elongation of the plasma cross-section allow ℓ_i to be determined from magnetics alone.

It is expected that more detailed information could be deduced in a more shaped plasma, such as a stellarator. The other-side of this argument is that the knowledge of ℓ_i is required to maintain the elongation in the shaped tokamak. This work will need to be done early in the conceptual design as many such diagnostics are often integral to the device itself and cannot be added after the fact. The results here indicate we will want to obtain an many moments as possible for the pressure and current profiles. Additionally, balanced injection is essential, otherwise, the central iota is depressed by NBCD leading to a double-valued iota profile with central iota rising above 1/2.

References:

[1] W.A. Houlberg, et.al., Phy. Plasmas **4** (1997) 3230.
[2] D.P. Schissel, et.al**.,** Nucl. Fus **31** (1991) 73.
[3] E. Sallander, et.al., Nucl. Fus **40** (2000) 1500.